PHYSICAL REVIEW C VOLUME 40, NUMBER 3 SEPTEMBER 1989

Interacting gluon model for hadron-nucleus and nucleus-nucleus collisions in the central rapidity region

G. N. Fowler
Department of Physics, University of Exeter, Exeter, United Kingdom

F. S. Navarra
Department of Physics, University of Marburg, Marburg, Federal Republic of Germany

M. Plümer
Department of Physics, University of Marburg, Marburg, Federal Republic of Germany
and Lawrence Berkeley Laboratory, Nuclear Science Division, Berkeley, California 94720

A. Vourdas
Department of Electrical Engineering and Electronics, University of Liverpool, Liverpool, United Kingdom

R. M. Weiner
Department of Physics, University of Marburg, Marburg, Federal Republic of Germany

G. Wilk
Solton Institute for Nuclear Studies, Warsaw, Poland
and Department of Physics, University of Marburg, Marburg, Federal Republic of Germany
(Received 22 December 1988)

The interacting gluon model developed to describe the inelasticity distribution in hadron-nucleon collisions has been generalized and applied to hadron-nucleus and nucleus-nucleus interactions. Leading particle spectra and energy distributions in hadron-nucleus and nucleus-nucleus collisions are calculated.

I. INTRODUCTION

One of the main challenges which high-energy heavy-ion physics is faced with at present is the determination of the energy density ε achieved in heavy-ion reactions.[1] It is clear that it is not enough to provide a mean value for $\varepsilon, \bar{\varepsilon}$, but the *distribution* of $\varepsilon, \chi(\varepsilon)$ is needed, in order to estimate the probability of exceeding a certain critical value ε_c, necessary, e.g., to achieve a quark-gluon plasma (QGP). So far apparently only $\bar{\varepsilon}$ has been calculated and even this number is obtained under assumptions which have not been subjected to an experimental test. Thus, e.g., one usually assumes the existence of a rapidity plateau in nucleus-nucleus (AA) collisions, one takes the energy density proportional to transverse energy density, and one assumes that nucleus-nucleus collisions can be reduced to a linear superposition of nucleon-nucleon reactions. Furthermore, most nucleon-nucleon inputs used so far do not distinguish between the central rapidity region and the fragmentation region.

In this paper we present an extension of the interacting gluon model, developed previously to describe the inelasticity and leading particle spectra in hadron-nucleon (hN) collisions,[2–4] to hadron-nucleus (hA) and nucleus-nucleus collisions. As before, our model applies only to the central rapidity region. This region is of special interest among other things because (i) at very high energies it is believed to contain most of the deposited energy and (ii) present folklore assumes that it is due mostly to gluons which are easier to handle in lattice quantum chromodynamics (QCD) calculations.

Apart from its relevance to the problem of QGP formation in nuclear collisions, the inelasticity distribution serves as an essential ingredient for statistical models[5,6] of multiparticle production in high-energy hadronic collisions that distinguish between production in the central region and in the fragmentation regions. In those models, observables such as the multiplicity of secondary particles tend to depend on the energy-momentum deposited in the central region rather than on the total center-of-mass-system (c.m.s.) energy available, $\sqrt{s}$, and the distributions of these observables are considerably broadened by inelasticity fluctuations;[6,7] consequently, any serious analysis of, e.g., the multiplicity distribution $P(n)$ has to take into account[7] these effects. In fact, there exists experimental evidence[8,9] to suggest that in hadron-hadron collisions $P(n)$ indeed depends on the invariant mass M of secondaries after the leading particles have been excluded, rather than on $\sqrt{s}$.

In contrast, in models such as the Fritiof Model developed by the Lund Group,[10] or the dual parton model,[11] hadron-hadron collisions are assumed to produce two or more excited strings, which eventually fragment into secondary particles; within such a scenario, no compelling reason exists to single out leading hadrons in the first place, and *a priori* one would not expect the total multiplicity distribution to depend on the invariant mass M defined above.

The interacting gluon model not only offers an explanation of the leading particle effect[8,9] but also predicts[2,3] the energy dependence[7] of the inelasticity distribution; thus, it is to be hoped that future experiments along the lines of Refs. 8 and 9 will help to clarify the contribution of gluon interactions to hN, hA, and AA high-energy collisions.

Finally, we would like to emphasize that the interacting gluon model, since it concentrates on the process of energy-momentum deposition, contains far fewer parameters than the string models already mentioned, which include elaborate hadronization prescriptions. Moreover, results obtained from analytic and semianalytic expressions in our model are more transparent than the corresponding Monte Carlo results of, e.g., Fritiof or the dual parton model.

The organization of the paper is as follows: we start in Sec. II with a presentation of the interacting gluon model for the hN interaction case. In this section also, distributions of interest are defined and the basic parameters of the model are fixed by fitting to the available data on inelasticity, its energy dependence and leading particle (LP) spectra. Section III deals with the generalization of the model to the hA case. Two different schemes are considered here. This generalized model is then confronted with the data on LP on nuclei. The inelasticity distribution for nuclei is also presented there. Section IV deals with further generalizations along the previous lines to the case of AA collisions.

As an application the (initial) energy density deposited in the central region is calculated for AA reactions and compared with existing data. It allows one to extract the longitudinal size of the initial energy deposition region. Remarks and conclusions are contained in Sec. V.

II. INTERACTING GLUON MODEL FOR THE hN CASE

The interacting gluon model originates from the observation[5,6,12] that according to (perturbative) QCD: $\sigma_{qq} < \sigma_{qg} < \sigma_{gg}$, where σ_{qq}, σ_{qg}, and σ_{gg} are the interaction cross sections of a quark-quark, quark-gluon, and gluon-gluon pair, respectively. Assuming the same inequality to hold also for soft interactions one expects that in each event one has weakly interacting, throughgoing valence quarks and strongly interacting and almost stopped glue (all possible $q\bar{q}$ sea quarks are thus "converted" to equivalent gluons). Such a picture is consistent with possible chaotic, or turbulent properties of the non-Abelian gauge fields[13] (i.e., gluons) suggesting a more rapid dissipation of the kinetic energy of colliding gluonic clouds and its redistribution among collective excitations on a very short time scale. The valence quarks are then supposed to be responsible for the fragmentation regions and especially for the leading particles, while the interacting gluons produce an indefinite number of "minifireballs" (MF's) through gluon fusion. Those MF's eventually form a lump of (gluonic) matter which we shall call a central fireball (CF) (cf. Fig. 1).

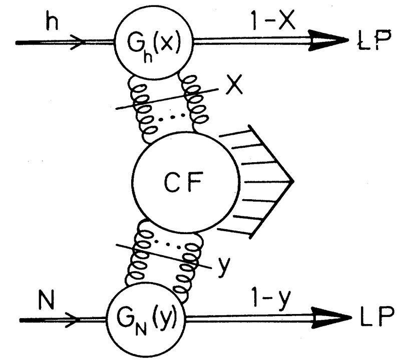

FIG. 1. Schematic view of the interacting gluon model. The notation is explained in the text.

In the present study we are interested only in the energy deposition in the central region. The question of particle distributions would require some model[14] to specify the conversion of the energy into particles and will not be discussed here. Because of this the actual form of a CF is not important for us and we shall assume in what follows that we have always only one CF. The other simplification will be the assumption that the energy not stored in the CF is to be found among produced LP's. (This overestimates the role of the CF in the cases where the central region is not yet fully developed; on the other hand, it makes our presentation more precise.)

Although the formalism of the model was presented previously, we have now introduced certain simplifications and therefore we present the main points again: We define the probability to form a CF by depositing fractions x and y of the energy momenta of the incoming hadrons as a sum over (an undefined number n of) MF's,

$$\chi(x,y)=\sum_{\{n_i\}}\delta\left[x-\sum_i n_i x_i\right]\delta\left[y-\sum_i n_i y_i\right]\prod_{\{n_i\}}P(n_i) \tag{1}$$

(all masses and transverse momenta are neglected in what follows[15]). The number distribution of MF's is given by $P(n_i)$ for which we use Poisson distributions

$$P(n_i)=\frac{\bar{n}_i^{\,n_i}\exp(-\bar{n}_i)}{n_i!} \tag{2}$$

corresponding to independent production. In this respect our approach resembles hadron or proton bremsstrahlung[16] models. As a matter of fact, it can be shown that the results for the inelasticity distribution are independent of the assumed form of $P(n_i)$ (cf. Appendix A). Expressing the delta functions via Fourier integrals one can perform all summations and arrive at the general formula:[18]

$$\chi(x,y)=\frac{1}{(2\pi)^2}\int_{-\infty}^{+\infty}dt\int_{-\infty}^{+\infty}du\,\exp\left[i(xt+yu)+\int_0^1 dx'\int_0^1 dy'\frac{d\bar{n}(x',y')}{dx'\,dy'}(e^{-i(x't+y'u)}-1)\right], \tag{3}$$

where we made a substitution

$$\sum_i \bar{n}_i(\cdots) \to \int_0^1 dx' \int_0^1 dy' \frac{d\bar{n}(x',y')}{dx'\,dy'}(\cdots) . \quad (4)$$

The central ingredient in our model is the spectral function of produced MF's, $\omega(x,y)=d\bar{n}/dx\,dy$, i.e., the mean number of MF's at given x and y which is proportional to the number of gg interactions. It reads

$$\omega(x,y)=\frac{\sigma_{gg}(\hat{s})}{\sigma_{hN}^{\text{in}}(s)}G_h(x)G_N(y)\Theta(xy-K_{\min}^2) ; \quad (5)$$

σ_{gg} and σ_{hN}^{in} are the inelastic gluon-gluon and hadron-nucleon cross sections, respectively, and $\hat{s}=M^2$, M being the invariant mass of the MF. The $G_{h,N}$ are the effective number of gluons which we approximate by the gluonic structure functions of corresponding hadrons normalized to the percentage of hadronic momentum allocated to the glue

$$\int_0^1 dx\, xG_{h,N}(x)=p_{h,N} . \quad (6)$$

The energy W and momentum P of the CF in the c.m. frame of hN are

$$W=\frac{\sqrt{s}}{2}(x+y),\quad P=\frac{\sqrt{s}}{2}(x-y) , \quad (7)$$

and its invariant mass M and rapidity Δ are

$$M=(W^2-P^2)^{1/2}=\sqrt{xys} ,$$
$$\Delta=\tfrac{1}{2}\ln\frac{W+P}{W-P}=\tfrac{1}{2}\ln\frac{x}{y} . \quad (8)$$

Here $\sqrt{s}$ is the total invariant energy of the reaction. The inelasticity of the reaction is then defined (in an invariant way) as

$$K=\frac{M}{\sqrt{s}}=\sqrt{xy} . \quad (9)$$

In this notation $K_{\min}$ is the minimal inelasticity

$$K_{\min}=\frac{M_0}{\sqrt{s}} , \quad (10)$$

M_0 being the mass of the lightest possible CF, which in principle is a free parameter.

As for $\sigma_{gg}(\hat{s})$, the simplest form (neglecting threshold effects when $M\to M_0$) which incorporates the most general energy dependence of the cross section, is

$$\sigma_{gg}(\hat{s}=M^2)=\frac{\alpha}{M^2}+\tilde{\delta}\ln\frac{M^2}{M_0^2} . \quad (11)$$

We have then two more parameters, α and $\tilde{\delta}$.

Because of the form of $G_{h,N}$, the spectral function $\omega(x,y)$ is sharply peaked at small (x,y) which justifies the approximation

$$\exp[-i(xt+yu)]-1\simeq -i(xt+yu) -\tfrac{1}{2}(xt+yu)^2 . \quad (12)$$

This leads to an analytic formula for $\chi(x,y)$,

$$\chi(x,y)=\frac{\chi_0}{2\pi(D_{xy}^2)^{1/2}}\exp\left\{-\frac{1}{2D_{xy}^2}[\langle y^2\rangle(x-\langle x\rangle)^2+\langle x^2\rangle(y-\langle y\rangle)^2-2\langle xy\rangle(x-\langle x\rangle)(y-\langle y\rangle)]\right\} , \quad (13)$$

where

$$\langle x^n y^m\rangle=\int_0^1 dx\, x^n\int_0^1 dy\, y^m\omega(x,y) \quad (14)$$

are (unnormalized) moments of the MF spectral function,

$$D_{xy}^2=\langle x^2\rangle\langle y^2\rangle-\langle xy\rangle^2 \quad (15)$$

and χ_0 is the normalization constant so that

$$\int_0^1 dx\int_0^1 dy\, \Theta(xy-K_{\min}^2)\chi(x,y)=1 . \quad (16)$$

One should mention here that Eq. (13) can be also derived using the saddle-point integration method in which one has a better control over the approximations involved. It can then serve as a starting point for possible improvements. The details of such an approach are presented in the Appendix B.

The (normalized) distribution $\chi(x,y)$ is our basic starting point. Out of it one can form all other distributions of interest. In the following we shall use the inelasticity distribution

$$\chi(K)=\int_0^1 dx\int_0^1 dy\, \Theta(xy-K_{\min}^2)\delta(\sqrt{xy}-K)\chi(x,y)$$
$$=2K\int_{K^2}^1\frac{dx}{x}\chi\left[x,\frac{K^2}{x}\right] \quad (17)$$

and the leading particle spectrum

$$f(x_L)=\int_0^1 dx\int_0^1 dy\, \Theta(xy-K_{\min}^2)\delta(1-x-x_L)\chi(x,y)$$
$$=\int_{K_{\min}^2/(1-x_L)}^1 dy\, \chi(1-x_L;y) ;$$
$$\chi_l\subset(0,\ 1-K_{\min}^2) , \quad (18)$$

where x_L is the fractional momentum of the LP.

All the relevant moments can now be easily evaluated. In Fig. 2 and Table I we present a sample of results

$$\langle\cdots\rangle\equiv\int_0^1 dx\int_0^1 dy\, \Theta(xy-K^2)(\cdots)\chi(x,y) .$$

Notice that $\langle\Delta\rangle=0$. The only experimental information about $\chi(K)$ available at present is that extracted from Ref. 8 (cf. Ref. 7). It is seen from Fig. 2(a) that the shape

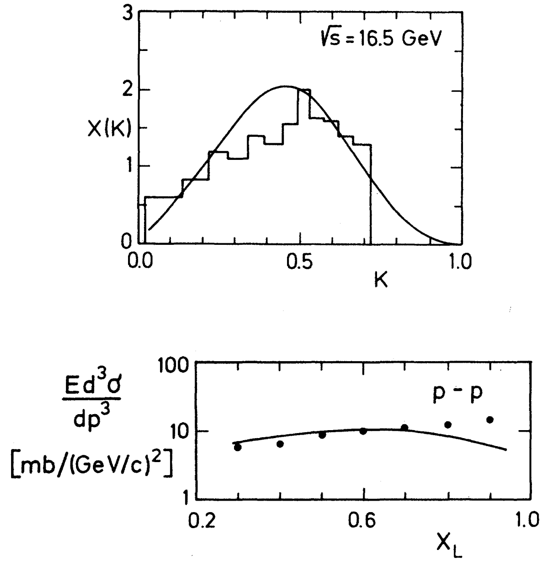

FIG. 2. (a) $\chi(K)$ for $\sqrt{s}=16.5$ GeV; the data are extracted from Ref. 8 (cf. Ref. 7). (b) Leading particle spectrum for $\sqrt{s}=14$ GeV (the data are from Ref. 19). The parameters are the same as for Table I, $\sigma_{pp}^{\rm in}=31$ mb.

of $\chi(K)$ at $\sqrt{s}=16.5$ GeV can be accounted for quite satisfactorily by the present approach.

Here and in what follows we use the simple structure function form[21]

$$G(x)=\frac{p(1+n)}{x}(1-x)^n\ , \tag{19}$$

which can readily be generalized to nuclear collisions (we use $n=5$). The values for $\langle K\rangle$ at $\sqrt{s}=16.5$ and 540 GeV in Table I were used as input. The parameters of the problem are M_0, which fixes our phase space and a combination of α and p in the form αp^2.

Because of the inequalities

$$\langle xy\rangle \ll \langle x^2\rangle < \langle x\rangle\ , \tag{20}$$

TABLE I. Results for different moments of χ for different energies. The parameters used are $M_0=0.35$ GeV, $\alpha p^2=0.036$ GeV^2 fm^2, $\tilde{\delta}=0$. The inelastic proton-proton cross sections used are $\sigma_{pp}^{\rm in}=31$, 56, 73, and 126 mb at $\sqrt{s}=16.5$ and 540 GeV and 2 and 40 TeV, respectively (Ref. 20). $D(\cdots) = \langle(\cdots)^2\rangle-\langle\cdots\rangle^2)^{1/2}$.

$\sqrt{s}$ (GeV)	$\langle K\rangle$	$\langle K^2\rangle$	$D(K)$	$D(\Delta)$
16.5	0.45[a]	0.24	0.18	0.24
540	0.30[a]	0.11	0.14	0.33
2 000	0.24	0.07	0.11	0.37
40 000	0.16	0.03	0.08	0.44

[a]Input.

we effectively deal with a Gaussian-like distribution $\chi(x,y)$:

$$\chi(x,y)\simeq \exp\left[-\frac{(x-\langle x\rangle)^2}{2\langle x^2\rangle}-\frac{(y-\langle y\rangle)^2}{2\langle y^2\rangle}\right]\ . \tag{21}$$

The energy dependence of $\chi(x,y)$ can be traced back to the energy dependence of σ_{gg} and in particular to the relative importance of the two different terms in σ_{gg} (decreasing and increasing with s, correspondingly). To estimate in a first approximation this energy dependence we keep only the $1/x$, $1/y$ terms in the structure functions and perform the integrations over the phase space [Eq. (14)]. Retaining only the leading terms in $\sqrt{s}$ one gets for the moments of the MF spectral function

$$\langle x\rangle \simeq 2\langle x^2\rangle \simeq \frac{\alpha}{M_0^2\sigma_{hN}^{\rm in}(s)}+\frac{\delta \ln^2\left[\frac{s}{M_0^2}\right]}{2\sigma_{hN}^{\rm in}}\ . \tag{22}$$

It is then clear that in order to have $\langle K\rangle$ or $\langle x\rangle$ decreasing with $\sqrt{s}$ (Ref. 22) we had to put $\tilde{\delta}=0$. Notice that, because both $\langle x\rangle$ and $\langle x^2\rangle$ decrease with s, we expect asymptotically,

$$\chi(x,y)\to\delta(x-\langle x\rangle)\delta(y-\langle y\rangle)\ ,$$
$$s\to\infty\ .$$

One should stress again that this refers only to the energy stored in the central region of rapidity. The actual measured distribution can (and will) be affected by contamination coming from the fragmentation regions (from the tails of the LP spectra in our case).[23]

III. EXTENSION TO hA COLLISIONS

Proceeding to hA and AA collisions one has to decide how to treat the nucleus. Different approaches were developed for this purpose.[24] Being an extended object, the nucleus is sensitive to the space time development and coherence properties of the scattering process, i.e., those aspects, which usually are not properly considered (if at all) in the process of model building of reaction mechanisms at the hadron-nucleon level. This implies, that new, previously unknown (or ignored) parameters appear, making a real differentiation between models very difficult.[24]

Recently, interest in the nuclear scattering problem has been renewed by the search for QGP.[1] From the data on hadron-nucleus leading particle spectra[19,25,26] information on the "stopping power" of the nucleus was extracted (in a model dependent way, however, and without specifying where the energy lost by the LP is deposited).[27]

Actually our model, although oversimplified, provides a clear answer to this question (at least for hA collisions): the energy goes into the CF occupying the central region in rapidity. (Furthermore, it will be seen in Sec. IV that recent AA collision data may provide some information on the size of this CF).

We shall proceed in the hA case, as in the hN case by considering particularly the role of gluonic sources in the deposition of energy leading to a CF. The most natural and straightforward generalization to nuclear processes is to treat the nucleons as an effective impact parameter (b) dependent, collective source composed of ν nucleons, and we shall use this method in the following.

This can be done in two ways which we shall call model (A) and model (B), respectively.

Model (A). This is a straightforward generalization of hN collisions to h-(νN) collisions where the (νN) cluster is treated as a single object [cf. Fig. 3(a)]. If $x,y \subset (0,1)$ the fractions of momenta of the incoming hadron and (νN) cluster in the hN c.m. frame, then the corresponding distribution $\chi_\nu(x,y)$ for a $h+(\nu N)$ collision is given by Eqs. (1)–(6) with the following substitutions:

$$\begin{aligned}
&(\text{i})\ M^2 \rightarrow M_\nu^2 = \nu x y s\ ,\\
&(\text{ii})\ W \rightarrow W_\nu = \frac{\sqrt{s}}{2}(x+\nu y)\ ,\\
&(\text{iii})\ P \rightarrow P_\nu = \frac{\sqrt{s}}{2}(x-\nu y)\ ,\\
&(\text{iv})\ G_N(y) \rightarrow G_\nu(y)\ ,\\
&(\text{v})\ \sigma_{hN}(s) \rightarrow \sigma_{\nu N}(\nu s)\ .
\end{aligned} \tag{23}$$

As mentioned previously all masses are neglected: $\sqrt{s}$ is the hN c.m. energy, $G_\nu(y)$ and $\sigma_{\nu N}(\nu s)$ are new (nuclear) quantities which are specified as follows: $G_\nu(y)$ represents the effective number of gluons in the struck ν-nucleonic cluster. We can expect that $G_\nu \sim \nu G_N$ and that $\int_0^1 dy\, y G_\nu(y) = p_\nu$, where p_ν is the percentage of the cluster momentum carried by gluons (we do not expect p_ν to differ drastically from $p_{\nu=1}=p$). This leads to

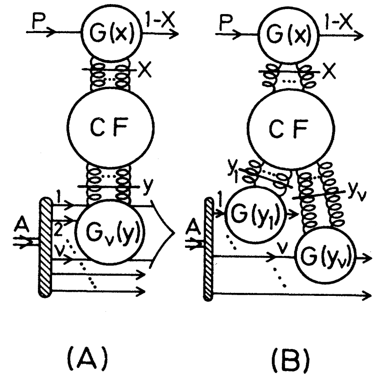

FIG. 3. Schematic view of the interacting gluon model for pA collisions. For notations cf. the text.

$$G_\nu(y) = \frac{\nu p_\nu(n+1)}{y}(1-y)^{\nu(n+1)-1}\ ;$$

$\sigma_{\nu N}$ represents the hadron-(νN) cluster cross section. From geometrical considerations it should not be very different from the hadron-nucleon case. Therefore, we take

$$\sigma_{\nu N} = \gamma \sigma_{hN} \quad (\gamma \sim 1)\ , \tag{24}$$

where γ is a new parameter.

Model (B). Here the incoming hadron collides again with ν nucleons inside the nucleus but they act now independently [cf. Fig. 3(b)]. The probability to form a CF by depositing fractions x and $y_1, \ldots, y_\nu$ of the energy momenta of the incoming hadron and nuclear nucleons involved in this collision is then

$$\chi_\nu(x;y_1,\ldots,y_\nu) = \sum_{\{n_{1i}\}\cdots\{n_{\nu i}\}} \delta\left[x - \sum_i \left[\sum_{l=1}^{\nu} n l_i\right] x_i\right] \prod_{l=1}^{\nu} \delta\left[y_l - \sum_i n_{l_i} y_{l_i}\right] \prod_{l=1}^{\nu} \prod_{\{n_{l_i}\}} P(n_{l_i})\ , \tag{25}$$

where the sum extends over the (undefined numbers of) MF's. Assuming as before a Poisson distribution for $P(n_i)$ and proceeding in an analogous way as in Sec. II, we arrive finally at an expression equivalent to Eq. (3):

$$\chi_\nu(x;y_1,\ldots,y_\nu) = \frac{1}{(2\pi)^{\nu+1}} \int_{-\infty}^{+\infty} dt\, e^{ixt} \prod_{l=1}^{\nu} \int_{-\infty}^{+\infty} du_l e^{iy_l u_l} \exp\left[\int_0^1 dx' \int_0^1 dy' \frac{d\bar{n}}{dx'\,dy'} (e^{-i(x't+y'u_l)} - 1)\right]\ . \tag{26}$$

Now the energy W_ν and momentum P_ν of the CF corresponding to h-(νN) collisions are

$$W_\nu = \frac{\sqrt{s}}{2}\left[x + \sum_{l=1}^{\nu} y_l\right],\quad P_\nu = \frac{\sqrt{s}}{2}\left[x - \sum_{l=1}^{\nu} y_l\right]\ , \tag{27}$$

and the invariant mass M_ν and rapidity Δ_ν,

$$M_\nu = \left[\left[x \sum_{l=1}^{\nu} y_l\right] s\right]^{1/2} \quad \Delta_\nu = \tfrac{1}{2}\ln \frac{x}{\sum_{l=1}^{\nu} y_l}\ . \tag{28}$$

Proceeding further as in Sec. II we finally get an analytical form for $\chi_\nu(x;y_1,\ldots,y_\nu)$:

$$\chi_\nu(x;y_1,\ldots,y_\nu)=\frac{\chi_{\nu 0}}{[(2\pi)^{\nu+1}\nu D_{xy}^2\langle y^2\rangle^{\nu-1}]^{1/2}}\exp\left[-\frac{\sum_{l=1}^{\nu}(y_l-\langle y\rangle)^2}{2\langle y^2\rangle}\right]$$
$$\times\exp\left\{-\frac{\left[(x-\nu\langle x\rangle)\langle y^2\rangle-\langle xy\rangle\sum_{l=1}^{\nu}(y_l-\langle y\rangle)\right]^2}{2\nu\langle y^2\rangle D_{xy}^2}\right\}, \quad (29)$$

where all definitions and the parametrization of $\langle x^n y^m\rangle$ and D_{xy}^2 are as in Sec. II [Eqs. (14) and (15)]; $\chi_{\nu 0}$ is the normalization constant (all χ_ν are separately normalized to 1). Notice that for $\nu=1$ we recover the result for the hN case, Eq. (13).

As we are interested only in the total energy-momentum transfer from the nucleus to the CF: $y=y_1+\cdots+y_\nu$, we now have to integrate over $\{y_l\}$ to get

$$\chi_\nu(x,y)=\int_0^1 dy_1\cdots\int_0^1 dy_\nu\,\delta\left[y-\sum_{l=1}^{\nu}y_l\right]\chi_\nu(x;y_1,\ldots,y_\nu). \quad (30)$$

That is our basic formula from which all relevant distributions will be calculated. Notice that although $\chi_\nu(x;y_1,\ldots,y_\nu)$ has a rather simple form, $\chi_\nu(x,y)$ cannot be obtained analytically as in model (A). The cross section $\sigma_{\nu N}$ is given again by Eq. (24).

We must also introduce the nuclear weight functions, P_ν^A, necessary for the averaging over the impact parameter

$$\chi_A(x,y)=\sum_{\nu=1}^{A}P_\nu^A\chi_\nu(x,y). \quad (31)$$

P_ν^A is the probability that the incoming nucleon strikes ν nucleons in the target A. We use for it a distribution which follows either from geometrical considerations,[28] or, as a limiting case for large A, from the Glauber model:[29]

$$P_\nu^A=\frac{1}{\nu!\sigma_{\text{in}}^{hA}}\int d^2b[n(b)]^\nu e^{-n(b)} \quad (32)$$

with $n(b)$ being the mean number of struck nucleons at a given impact parameter b

$$n(b)=\sigma_{\nu N}\int_{-\infty}^{+\infty}dz\,\rho(\mathbf{b},z) \quad (33)$$

and

$$\sigma_{hA}^{\text{in}}=\int d^2b(1-e^{-n(b)}). \quad (34)$$

$\rho(\mathbf{b},z)$ is the nuclear number density normalized to A. (In what follows we have adopted for our NA calculations the ρ used by Date *et al.*[27])

The parameters of the problem are now, in model (A)—M_0, γ, and a combination of α, p_ν, and p under the form $\alpha p_\nu p$; in model (B)—M_0, γ, and a combination of α and p under the form αp^2. The values for M_0 and αp^2 were taken from the pp case. Then it turns out that models (A) and (B) give very similar results if one chooses $\alpha p_\nu p=\alpha p^2$ and $\gamma=1.15$ in model (A) (Ref. 30) and $\gamma=1$ in model (B), cf. Fig. 4 and Table II. Therefore, in what follows, only results for model (A) will be shown. Figs. 4–6 represent a comparison of our calculations with different data on LP distributions. In Fig. 7 the mean number of slow protons calculated with our prescription for P_ν^A is compared with data. In Fig. 8 our predictions for the inelasticity distributions for different nuclei are presented.

The LP spectrum is now for model (A) [cf. Eq. (18)]

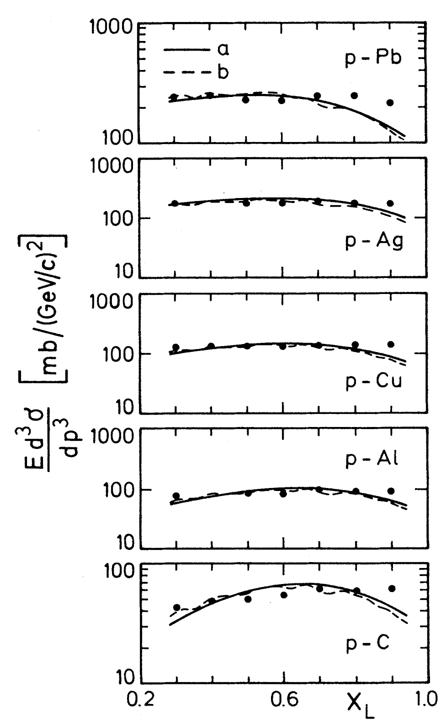

FIG. 4. Leading particle spectrum for various nuclei. The data are from Ref. 19 (for fixed $p_T=0.3$ GeV/c). The parameter values used are $M_0=0.35$ GeV, $\alpha p p_\nu=0.036$ GeV^2 fm^2, and $\gamma=1.15$ for model (A), full line, and $\gamma=1$ for model (B), dashed line (the irregularities are caused by Monte Carlo integration).

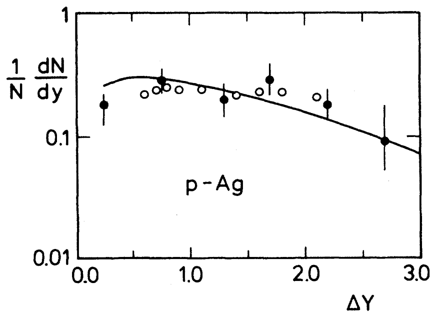

FIG. 5. The leading particle spectrum for p-Ag reaction, data points are from Refs. 25 and 26. They cover a wider range of rapidity loss of the leading particle $\Delta y \sim -\ln x_L$ than those of Ref. 19. The parameters used are the same as in Fig. 4.

$$f_A(x_L)=\sum_{\nu=1}^{A} P_\nu^A \int_{K_{\min}^2/[\nu(1-x_L)]}^{1} dy\, \chi_\nu(1-x_L,y) \times\Theta\left[1-x_L-\frac{K_{\min}^2}{\nu}\right], \tag{35}$$

and for model (B)

$$f_A(x_L)=\sum_{\nu=1}^{A} P_\nu^A \int_0^1 dx \prod_{l=1}^{\nu}\int_0^1 dy_l \Theta(xy_l-K_{\min}^2) \times\delta(1-x-x_L) \times\chi_\nu(x;y_1,\ldots,y_\nu). \tag{36}$$

($K_{\min}=M_0/\sqrt{s}$ as before, $\sqrt{s}$ is the nucleon-nucleon c.m. energy). The inelasticity distribution is, correspondingly for model (A) [cf. Eq. (17)],

$$\chi_A(K)=2KA\sum_{\nu=1}^{A} P_\nu^A \Theta\left[\sqrt{\nu/A}-K\right]\Theta\left[K-\frac{K_{\min}}{\sqrt{\nu}}\right]\frac{1}{\nu} \times\int_{AK^2/\nu}^{1}\frac{dx}{x}\chi_\nu\left[x,\frac{AK^2}{\nu x}\right], \tag{37}$$

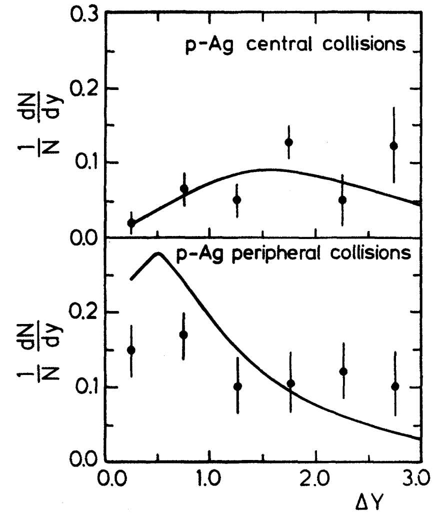

FIG. 6. The same data as in Fig. 5, but presented for the "central" and "peripheral" parts (cf. Ref. 26). In our calculations we set accordingly $6\le\nu\le10$ for the central part and $1\le\nu\le5$ for the peripheral one. Other parameters and notation are as in Fig. 5.

and for model (B)

$$\chi_A(K)=2KA\sum_{\nu=1}^{A} P_\nu^A \int_{K_{\min}^2}^{1} dx\left[\prod_{l=1}^{\nu}\int_{K_{\min}^2/x}^{1} dy_l\right] \times\delta\left[x-\frac{AK^2}{\sum_{l=1}^{\nu} y_l}\right] \times\left[\frac{\chi_\nu(x;y_1,\ldots,y_\nu)}{\sum_{l=1}^{\nu} y_l}\right], \tag{38}$$

where K is the ratio of the invariant energy deposited into the central region (the mass of the CF) to the total invariant energy of the reaction: $\sqrt{s_A}=\sqrt{As}$.

As may be seen, the fit to the LP spectra for pA is of the same quality as for pp. The theoretical results are always below the experimental ones at small x, i.e., large

TABLE II. Results for different moments of χ and for masses of CF for different nuclei. The parameters are the same as for Fig. 4. The incoming proton momentum is $p_{\rm lab}=100$ GeV/c.

	Model (A)				Model (B)			
	$\langle x\rangle$	$\langle K\rangle$	$\langle\sqrt{K}\rangle$	$\langle M\rangle$ (GeV)	$\langle x\rangle$	$\langle K\rangle$	$\langle\sqrt{K}\rangle$	$\langle M\rangle$ (GeV)
$p\,^{12}$C	0.56	0.17	0.39	7.9	0.60	0.20	0.44	9.5
$p\,^{27}$Al	0.59	0.13	0.35	9.5	0.62	0.15	0.37	10.7
$p\,^{63}$Cu	0.63	0.10	0.30	10.9	0.65	0.11	0.32	12.0
$p\,^{108}$Ag	0.65	0.08	0.28	12.2	0.67	0.09	0.29	13.6
$p\,^{207}$Pb	0.68	0.07	0.25	13.4	0.69	0.08	0.27	15.0

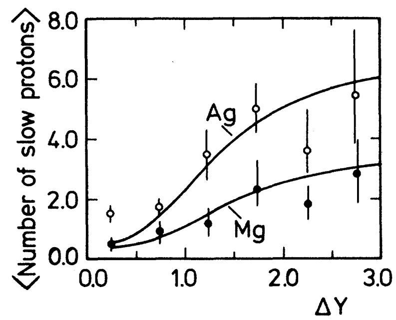

FIG. 7. Results for the number of slow protons (essentially given by $\bar{\nu}^2$, cf. Ref. 29) vs Δy; the notation and the parameters are as in Fig. 5. For $\bar{\nu}(\Delta y)$ we use the relation

$$\bar{\nu}(\Delta y)=\left[\sum_{\nu} \nu P_{\nu}^{A} \int dy\, \chi(1-x_L,y) \Big/ \sum_{\nu} P_{\nu}^{A} \int dy\, \chi(1-x_L,y)\right] ,$$

$$\Delta y \sim -\ln x_L .$$

x_L. This could be due either to the fact that the data contain contamination from other processes such as diffraction or that our treatment of the valence quarks components as *the* LP's is, perhaps, too strong an assumption, or both.

This is also reflected in Fig. 6 where it is seen that the model can account quite well for the "central collision" part but not for the "peripheral one." To be conservative it appears therefore preferable to limit the applications of our model to the central rapidity region. A clear experimental separation of the central and fragmentation regions which are determined by different dynamics would be of great value whenever possible.

The fact that our calculations for the number of slow protons observed agree rather well (Fig. 7) with data suggests that our model for P_{ν}^{A} is an adequate one.

In Table II the moments $\langle x \rangle$, $\langle K \rangle$, $\langle \sqrt{K} \rangle$, and $\langle M \rangle = \langle K \rangle \sqrt{s_A}$ for incoming proton momentum $p_{\rm lab}=100$ GeV/c are presented for both models (A) and (B). From $\langle x \rangle$ one can calculate the energy deposited in the laboratory frame using the formula $W_{\rm lab} \approx \langle x \rangle p_{\rm lab}$. Model ($B$) gives slightly higher values of inelasticities $\langle x \rangle$ and $\langle K \rangle$ [this is due to the different approach to the (νN) clusters in the two models; the LP spectra are practically the same for both models]. So far no measurements of $\chi_A(K)$ have been reported. There exist data[31] only for the transverse energy distribution $d\sigma/dE_T$. Unfortunately, E_T is a highly model-dependent function of the invariant energy deposited M_A, so that we cannot use it for comparison with our results. The only piece of experimental information on inelasticity are the results from cosmic ray data[32] where the A dependence of the energy $W_{\rm lab}$ deposited in the laboratory frame by the projectile was found to be $A^{0.06\pm0.04}$. Our result is $\langle x \rangle \sim A^{0.07}$ for model (A) and $\langle x \rangle \sim A^{0.05}$ for model (B).

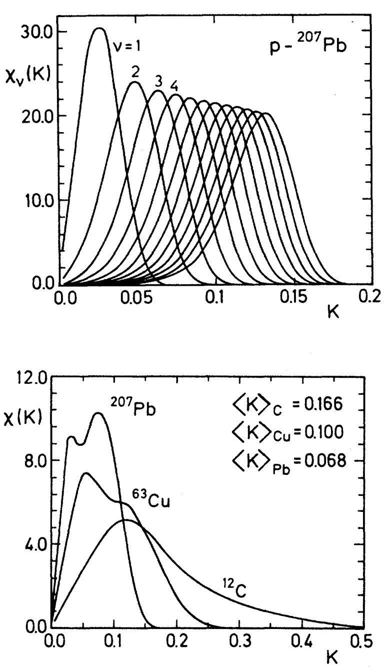

FIG. 8. (a) Example of $\chi_\nu(K)$ for $p\,^{207}$Pb collision; (b) Inelasticity distribution $\chi_A(K)$ for $A=12$, 63, and 207. In both cases the incoming nucleon momentum $p_{\rm lab}=100$ GeV/c and the parameters are as in Fig. 4. The corresponding values of $\langle M_A \rangle = \langle K_A \rangle \sqrt{s}$ are given in Table II.

IV. AA COLLISIONS IN THE INTERACTING GLUON MODEL

Both models (A) and (B) can be generalized to AA collisions in a straightforward way. On the other hand, because of the complexity of model (B) we shall present numerical results obtained only for model (A). However, for completeness we provide in Appendix C the corresponding formulae of model (B), too.

A generalization of our approach to AA collisions in model (A) can be obtained as follows. We regard the collision as taking place between a (μ-nucleonic) object from one nucleus (A) on a (ν-nucleonic) system from the other one (B). The corresponding $\chi_{\mu\nu}(x,y)$, calculated as before in the NN c.m. frame is again given by Eqs. (1)–(6); as before all masses are neglected; $\sqrt{s}$ is the NN c.m. energy. Relations (23) are now replaced by

$$\text{(i)}\ M^2 \to M_{\mu\nu}^2 = \mu\nu x y s ,$$

$$\text{(ii)}\ W \to W_{\mu\nu} = \frac{\sqrt{s}}{2}(\mu x + \nu y) ,$$

$$\text{(iii)}\ P \to P_{\mu\nu} = \frac{\sqrt{s}}{2}(\mu x - \nu y) , \qquad (39)$$

$$\text{(iv)}\ G_h(x) \to G_\mu(x), \quad G_N(y) \to G_\nu(y) ,$$

as defined in Sec. III

$$\text{(v)}\ \sigma_{hN} \to \sigma_{\mu\nu} = \gamma' \pi r_0^2 (\mu^{1/3} + \nu^{1/3})^2 .$$

The parameters of the problem are now M_0 and a combination of α, p_μ, p_ν, and γ' under the form $\xi = \alpha p_\mu p_\nu / \gamma'$

where we expect (as in the previous case) that $\gamma' \sim \gamma \sim 1$ and $p_\nu \simeq p_\mu \simeq p$. To calculate

$$\chi_{AB}(x,y) = \sum_{\mu=1}^{A} \sum_{\nu=1}^{B} P_{\mu\nu}^{AB} \chi_{\mu\nu}(x,y) , \tag{40}$$

we must now specify the probabilities $P_{\mu\nu}^{AB}$ of encountering (μ,ν)-nucleonic combinations of the colliding objects. This we do in a simple geometrical model, with both nuclei taken as rigid spheres of radii $R = r_0 A^{1/3}$ and number density $\rho = 0.17\ \mathrm{fm}^{-3}$. For each impact parameter b we can then calculate the number of participating nucleons $\mu = \mu(b)$ (from A) and $\nu = \nu(b)$ (from B) by just counting the number of nucleons in the corresponding overlapping volumes (in b space) $V_{A,B}(b)$:

$$V_A(b) = 2\int d^2s [R_A^2 - (\mathbf{s}-\mathbf{b})^2]^{1/2} \times \Theta[R_A^2 - (\mathbf{s}-\mathbf{b})^2]\Theta(R_B^2 - \mathbf{s}^2) \tag{41}$$

and similarly for $V_B(b)$.[33] Then $\mu(b) = \rho V_A(b)$ and $\nu(b) = \rho V_B(b)$.

Because of the one-to-one correspondence between the number of participants $\mu+\nu$ and the impact parameter b of the reaction, Eq. (40) becomes

$$\chi_{AB}(x,y) = \int d^2b\, f(b) \chi_{\mu(b)\nu(b)}(x,y) \tag{42}$$

with the weight factor $f(b)$ being equal to

$$f(b) = \frac{1}{\sigma_{AB}} \frac{b\Delta(b)}{R_{AB}^2} , \tag{43}$$

where $R_{AB} = R_A + R_B$ and σ_{AB} is the nucleus-nucleus total inelastic cross section which we take to be $\sigma_{AB} = \pi R_{AB}^2$. $\Delta(b)$ is the increment of impact parameter b leading to an increase of the number of participants, $\mu+\nu$, by unity [actually from $(\mu+\nu-\frac{1}{2})$ to $(\mu+\nu+\frac{1}{2})$], such that $\int d^2b\, f(b) = 1$. Now our interacting gluon model for AA collisions is fully specified. Actually the simplified weight factor $f(b) = 1/\sigma_{AB}$ leads to the same numerical results. This is so because the region of b where differences occur (i.e., $b \to R_A + R_B$) is excluded by the experimental cuts (it corresponds to very small E_T).

As in the NA case in most experiments only $d\sigma/dE_T$ has been measured (Refs. 34–36), cf. also "Quark Matter '87," Ref. 1), so that the qualification made in Sec. III applies here, too. However, in the WA-80 experiment[34] the initial local energy density ε is also provided by using the relation (where τ_0 is an initial proper time for imposition of boundary conditions for hydrodynamical flow) (Ref. 37)

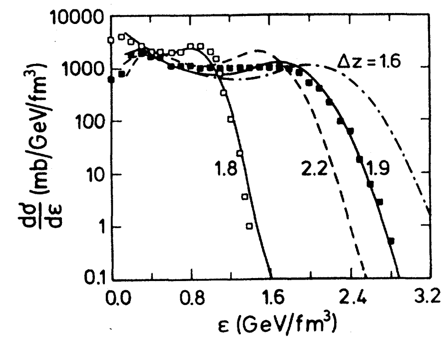

FIG. 9. Comparison with energy density from Ref. 34. The value of ξ is 0.026 $\mathrm{GeV}^2\,\mathrm{fm}^2$.

$$\varepsilon = \frac{1}{\pi R^2 \tau_0} \frac{dE_T}{dy} \tag{44}$$

with $\tau_0 = 1$ fm and $R = R(^{16}\mathrm{O}) = 3.0$ fm.

In our approach we can *directly* determine the (global) energy density:[38]

$$\tilde{\varepsilon} = \frac{M_{AB}}{\pi R^2 \Delta z} , \tag{45}$$

where $M_{AB} = K\sqrt{s_{AB}}$ is the invariant energy deposited into the CF ($\sqrt{s_{AB}}$ being the total invariant energy of the AB collision, K the inelasticity defined with respect to this energy), and Δz is the longitudinal dimension of the CF in its rest frame (which for all practical purposes can be identified with the NN c.m. frame where the calculations of M_{AB} are performed). In our approach (as in all other approaches) this is a free parameter which we shall determine as follows. We assume that $\tilde{\varepsilon} = \varepsilon$ and identify the ε distribution $d\sigma/d\varepsilon$ measured in Ref. 34 with the $\tilde{\varepsilon}$ distribution given by our calculation, i.e., with

$$\frac{d\sigma}{d\tilde{\varepsilon}} = \mathrm{const}\,\chi(\tilde{\varepsilon}) . \tag{46}$$

Keeping the value of the parameter M_0 the same as for the pp case we have then two parameters: ξ and Δz which are obtained from a best fit. In Fig. 9 we show the results of such a fit corresponding to

$$\chi_{AB}\left[K = \frac{\pi R^2 \Delta z}{\sqrt{s_{AB}}}\tilde{\varepsilon}\right] = 2ABK \sum_{\mu=1}^{A} \sum_{\nu=1}^{B} P_{\mu\nu}^{AB} \Theta\left[K - \frac{K_{\min}}{\sqrt{AB}}\right] \Theta\left[\left[\frac{\mu\nu}{AB}\right]^{1/2} - K\right] \frac{1}{\mu\nu} \int_{K^2 AB/\mu\nu}^{1} \frac{dx}{x} \chi_{\mu\nu}\left[x, \frac{ABK^2}{\mu\nu x}\right] , \tag{47}$$

where $\Delta z = 1.9$ fm and $\xi = 0.026\ \mathrm{GeV}^2\,\mathrm{fm}^2$ [if one chooses $\alpha p_\mu p_\nu = \alpha p^2$ and takes this last quantity the same as for the pp case, this value of ξ corresponds to $\gamma' = 1.38$ in Eq. (39)]. The fit is a rather sensitive function of the parameters (see Fig. 9), and for the values given above for ξ and Δz, it is quite good. This suggests that our approach can be used to estimate both the shape of $d\sigma/d\varepsilon$ and the value of Δz. We also find that in the present energy range ($60A$–$200A$ GeV) Δz is practically unchanged. From the above considerations it follows that Δz is the impact parameter averaged longitudinal dimension of the CF. The mean mass (averaged over b) of the

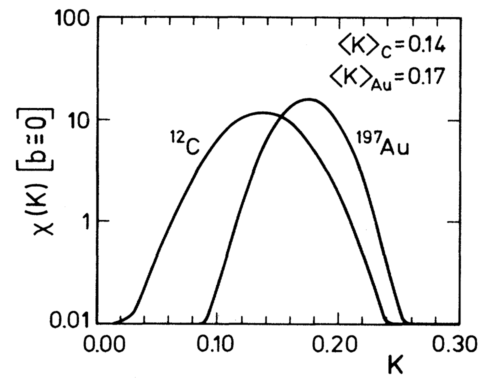

FIG. 10. The inelasticity distribution for $b=0$ [K is defined now with respect to the $\sqrt{s(b)}$ at $b=0$, cf. Table III]. The parameters are as in Fig. 9.

CF for the $^{16}O+{}^{197}Au$ collision at 200A GeV is

$$\langle M_{AB}\rangle = \sqrt{s_{AB}}\int_{K^2_{\min}}^{1} dK\, K\chi_{AB}(K) = 84 \text{ GeV} \quad (48)$$

and the mean energy density is $\langle\varepsilon\rangle = 1.56$ GeV/fm^3. On the other hand, for central collisions $\langle M_{AB}(b=0)\rangle = 140$ GeV and correspondingly $\langle\varepsilon(b=0)\rangle = 2.6$ GeV/fm^3 (assuming that Δz does not change very much with b).

We would like to stress here that our model providing directly the distribution of the total (invariant) energy deposited in the central region of rapidity is especially suited for an estimate of the energy density, if the volume is known, or of the volume of interaction $V=\pi R^2\Delta z$, if the energy density is known. In all other models used for nucleus-nucleus reactions[39] one assumes that AA collisions are just a superposition of NN collisions and there is no natural way to introduce a volume. This point of view, however, has been criticized because it is contradicted by many simple estimates and observations (cf. Ref. 40).

One should also bear in mind that the data of Ref. 34 which we have used, have not been corrected for longitudinal expansion. Equation (44) is only an approximation to the initial energy density since, after all, the data refer to the final state. The correction necessary to account for this can be done using the results of Ref. 41, but for the moment we shall accept Eq. (44), bearing in mind that it will lead to an overestimate of the initial Δz. It should also be added that the main condition of the application of Eq. (44), and of our method, is the separation of the central and fragmentation regions, which, at least at present energies is at best only approximately satisfied.

In Fig. 10 we present—as a prediction—$\chi[K(b=0)]$, i.e., the inelasticity distribution for central collisions, with K defined with respect to the available invariant energy $\sqrt{s(b=0)}=\sqrt{2\mu\nu p_{\text{lab}}}$ at this impact parameter. Table III summarizes the mean values of K and M in this case.[42]

V. DISCUSSION

We have shown that a model which used as input gluon-gluon interactions at nucleon-nucleon level can provide a satisfactory description of inelasticity distributions in nucleon-nucleon reactions, the leading particle spectrum in nucleon-nucleon and nucleon-nucleus reactions, and of the energy distribution in nucleus-nucleus reactions.

The main limitations of the present approach follow. (a) It is restricted to the central rapidity region. (b) It is based on a very simple geometrical interpretation of nuclear collective effects. Both these limitations can be overcome and work along these lines is in progress. However, the results obtained already are in our view interesting because they not only show that a collective reaction mechanism can be at work, but also because they provide the first distribution of initial energy density and the first estimate of the initial volume in heavy-ion reactions.

These quantities have not been determined so far by other models like the dual parton model[43] and the Lund model[44] which are often quoted in the literature, among other things, because they do not emerge in a natural way from these approaches, which are based on the idea of fragmentation of noninteracting strings. It is difficult to see how the energy stored in the central region can be calculated consistently in a string approach without allowing for an interaction between the strings, a point raised recently also by Shuryak in a different context.[40] As a matter of fact the statistical model of the Berlin group[45] comes closer to our approach in the sense that it also calculates the energy stored in the central region. However, this model, like all the other models quoted, neglects the momentum of the central fireball and therefore cannot calculate the *invariant* energy distribution which is a necessary ingredient for the determination of the energy density.

TABLE III. Mean values of inelasticity $\langle K\rangle$ and of the central fireball mass $\langle M\rangle$ for central collisions of ^{16}O on ^{12}C and ^{197}Au. The parameters for $^{16}O+{}^{197}Au$ collisions are obtained from the data on energy density as in Fig. 9. Because of the lack of such data for $^{16}O+{}^{12}C$ collisions, we used in this case the same parameters as in the collision of ^{197}Au. The number of participants from each nucleus is also shown together with the available invariant energy $\sqrt{s(b=0)}=\sqrt{2\mu\nu p_{\text{lab}}}$.

	$\langle K(b=0)\rangle$	$\mu_{b=0}$	$\nu_{b=0}$	$\sqrt{s(b=0)}$ (GeV)	$\langle M(b=0)\rangle$ (GeV)
$^{16}O+{}^{12}C$	0.14	15	12	268	37
$^{16}O+{}^{197}Au$	0.17	16	53	582	140

The first numerical estimate of initial longitudinal dimension of the order of 2 fm at 200 GeV/nucleon obtained here, with all its limitations is certainly of importance for future theoretical and experimental work. The energy distributions obtained in the present paper can be used among other things for the calculation of multiplicity and rapidity distributions, a subject which will be addressed in further publications.

ACKNOWLEDGMENTS

This work was funded in part by the German Minister for Research and Technology (BMFT) under Contract Number 06 MR 777 and the Conselho Nacional de Desenvolvimento Científico e Technológica (CNPq), Brazil. The work of M.P. has been supported by a Deutsche Forschungsgemeinschaft Postdoctoral Fellowship.

APPENDIX A: INELASTICITY FROM CHAOTIC SOURCES

Although we do not know in detail the dynamics of minifireball production, quantum statistics provides us with some constraints on their multiplicity distribution. The minifireballs are produced by sources which can be either coherent, chaotic, or of mixed distribution type.[17] The first case was already discussed in the text. Here we investigate the consequences of replacing the Poisson distribution [Eq. (2)] by a Bose-Einstein which is expected in the case of chaotic production.

Assuming that $P(n_i)$ has the form

$$P(n_i)=\frac{\bar{n}_i^{\,n_i}}{(1+\bar{n}_i)^{n_i+1}} \tag{A1}$$

and repeating the steps in the derivation of $\chi(x,y)$ we get

$$\chi(x,y)=\frac{1}{(2\pi)^2}\int_{-\infty}^{+\infty}dt\int_{-\infty}^{+\infty}du\; e^{i(xt+yu)} \times\exp\left\{-\sum_{j=1}^{N}\ln[1+\bar{n}_i(1-e^{-i(x_jt+y_ju)})]\right\}, \tag{A2}$$

where N is the number of cells in phase space.

Going now to the limit in which N is infinite and the size of each cell goes to zero, $\bar{n}_i$ is small (actually vanishing) everywhere except in a small region around the phase-space origin ($x\rightarrow 0$, $y\rightarrow 0$). Inside this region $\bar{n}_i$ could be large due to the divergent behavior of Eq. (5). However, in our case precisely this region of the phase space is cutoff by the condition $K>K_{\min}$ imposed on inelasticity K. As the function multiplying $\bar{n}_i$ oscillates between 0 and 1, one can then expand the $\ln\cdots$ term and (A2) becomes identical to [Eq. (3)] in Sec. II.

APPENDIX B: DERIVATION OF $\chi(x,y)$ BY THE SADDLE-POINT INTEGRATION METHOD

The accuracy of the approximations involved in the calculation of $\chi(x,y)$ can be improved if one applies the method of saddle-point integration. To implement this formalism, first replace the δ functions on the right-hand side (rhs) of Eq. (1) by the integral representations:

$$\delta\left[x-\sum_j n_jx_j\right]=\frac{1}{2\pi}\int_{-\infty}^{+\infty}d\alpha'\exp\left[\bar{\alpha}\left[x-\sum_j n_jx_j\right]\right],$$
$$\delta\left[y-\sum_j n_jy_j\right]=\frac{1}{2\pi}\int_{-\infty}^{+\infty}d\beta'\exp\left[\bar{\beta}\left[y-\sum_j n_jy_j\right]\right], \tag{B1}$$

where $\bar{\alpha}=\alpha+i\alpha'$, $\bar{\beta}=\beta+i\beta'$, and $\alpha,\alpha',\beta,\beta'$ are arbitrary real numbers. Carrying out now the sums and products in Eq. (B1) and going to the continuum limit as before, one immediately obtains

$$\chi(x,y)=\frac{1}{(2\pi)^2}\int_{-\infty}^{+\infty}d\alpha'\int_{-\infty}^{+\infty}d\beta'\exp[\bar{\alpha}x+\bar{\beta}y+F(\bar{\alpha},\bar{\beta})] \tag{B2}$$

with

$$F(\bar{\alpha},\bar{\beta})=\int_{K_{\min}^2}^{1}dx'\int_{K_{\min}^2/x'}^{1}dy'\frac{d\bar{n}(x',y')}{dx'dy'}\{\exp[-(\bar{\alpha}x'+\bar{\beta}y')]-1\}\;. \tag{B3}$$

[Note that one recovers Eq. (3) if one puts $\alpha=\beta=0$ in Eqs. (B2) and (B3)]. Expansion of the terms in the exponent on the rhs of Eq. (B2) to second order in α',β' around $\alpha'=\beta'=0$ yields

$$\bar{\alpha}x+\bar{\beta}y+F(\bar{\alpha},\bar{\beta})\approx\alpha x+\beta y+F(\alpha,\beta)+i(C_{10}+x)\alpha'+i(C_{01}+y)\beta'-\tfrac{1}{2}C_{20}(\alpha')^2-\tfrac{1}{2}C_{02}(\beta')^2-C_{11}\alpha'\beta'\;, \tag{B4}$$

where

$$C_{kl}\equiv\frac{\partial^{k+l}F(\bar{\alpha},\bar{\beta})}{\partial\bar{\alpha}^k\partial\bar{\beta}^l}=\int_{K_{\min}^2}^{1}dx'\int_{K_{\min}^2/x'}^{1}dy'(-1)^{k+l}x'^{k}y'^{l}\frac{d\bar{n}(x',y')}{dx'dy'}e^{-(\alpha x'+\beta y')}\;. \tag{B5}$$

Substitution of Eq. (B4) into Eq. (B2) permits an analytic evaluation of the integral on the rhs of Eq. (B2). However, for a given point (x,y) the approximation (B4) may be improved if $\alpha=\alpha(x,y)$ and $\beta=\beta(x,y)$ are chosen in such a way that the coefficients of the linear terms in α' and β' in (B4) vanish, i.e., α and β are required to satisfy the coupled equations:

$$x=\int_0^1 dx'\int_0^1 dy'\Theta(x'y'-K_{\min}^2)x'\frac{d\bar{n}}{dx'dy'}e^{-(\alpha x'+\beta y')}\,,$$
$$y=\int_0^1 dx'\int_0^1 dy'\Theta(x'y'-K_{\min}^2)y'\frac{d\bar{n}}{dx'dy'}e^{-(\alpha x'+\beta y')}\,. \tag{B6}$$

With this the final result is (modulo a normalization constant)

$$\chi(x,y)=\frac{1}{2\pi(C_{20}C_{02}-C_{11}^2)^{1/2}}\exp\left[\alpha x+\beta y+\int_0^1 dx'\int_0^1 dy'\Theta(x'y'-K_{\min}^2)\frac{d\bar{n}}{dx'dy'}(e^{-(\alpha x'+\beta y')}-1)\right]. \tag{B7}$$

It is easy to show that the earlier result, Eq. (13) is recovered from Eq. (B7) if one approximately solves (B6) for α,β by linearizing and expanding the functions $\exp[-\alpha x'-\beta y']x'^k y'^l$ in (B5) and (B7) up to second power in x' and/or y' around $x'=y'=0$.

APPENDIX C: MODEL (B) FOR AA COLLISIONS

Suppose that we have a situation in which in the scattering of two nuclei A and B, μ nucleons from A and ν nucleons from B participate in the collision. In order to write down $\chi_{\mu\nu}$ we need to know the minimal number n of MF's to start with [cf. Eq. (25)]. Contrary to the situation in NA scattering this number is now not fixed and can be

$$\max(\mu,\nu)\le n\le \mu\nu\,. \tag{C1}$$

The case $n=\mu\nu$ corresponds to the situation when each of the participating μ nucleons of A interacts with each of the participating ν nucleons of B (maximally inelastic event). The case $n=\max(\nu,\mu)$ corresponds to the situation when the number of MF's is just the minimally possible one.

Let us define the matrix

$$C_{kl}=\begin{cases}1 & \text{if nucleons } k \text{ and } l \text{ interact}\,,\\ 0 & \text{otherwise}\,.\end{cases} \tag{C2}$$

Obviously,

$$n=\sum_{k=1}^{\mu}\sum_{l=1}^{\nu}C_{kl}\,. \tag{C3}$$

Let x_{kl} be a fractional momentum of the nucleon k in nucleus A which collides with a nucleon l in nucleus B and y_{kl} be a fractional momentum of the nucleon l in nucleus B which collides with a nucleon k in the nucleus A. Then

$$x_k=\sum_{l=1}^{\nu}x_{kl}$$

is the total momentum loss of the nucleon k in nucleus A, and similarly

$$y_l=\sum_{k=1}^{\mu}y_{kl}$$

is the total momentum loss of the nucleon l in nucleus B. Let $n_i^{(kl)}$ be the number of gluon-gluon collisions of gluons with momenta $x_i^{(kl)}$ and $y_i^{(kl)}$ which come from the nucleons k and l. Let us finally assume that the probability of $n_i^{(kl)}$ such collisions is given by

$$P^{(kl)}[n_i^{(kl)}]=\begin{cases}\dfrac{[\bar{n}_i^{(kl)}]n_i^{(kl)}}{n_i^{(kl)}}\exp[-\bar{n}_i^{(kl)}] & \text{if } C_{kl}=1\,,\\ \delta_{0,n_i^{(kl)}} & \text{otherwise}\,.\end{cases} \tag{C4}$$

Then

$$\chi_{\mu\nu}(\{x^{(\mu)}\},\{y^{(\nu)}\})=\sum_{\{n_i^{(kl)}\}}\left[\prod_{i,k,l}P_i^{(kl)}(n_i^{(kl)})\right]\prod_{k-1}^{\mu}\delta\left[x^{(k)}-\sum_i\sum_{l=1}^{\nu}n_i^{(kl)}x_i^{(kl)}\right]\prod_{l=1}^{\nu}\delta\left[y^{(l)}-\sum_i\sum_{k=1}^{\mu}n_i^{(kl)}y_i^{(kl)}\right]. \tag{C5}$$

Using as before Fourier transform representations for the δ functions we can perform the corresponding summations and get

$$\chi_{\mu\nu}(\{x^{(\mu)}\},\{y^{(\nu)}\})=\frac{1}{(2\pi)^{\mu+\nu}}\prod_{k=1}^{\mu}\int_{-\infty}^{+\infty}dt_k\prod_{l=1}^{\nu}\int_{-\infty}^{+\infty}du_l\exp\left[i\sum_{k=1}^{\mu}t_kx^{(k)}+i\sum_{l=1}^{\nu}u_ly^{(l)}\right]$$
$$\times\exp\left[\sum_{k=1}^{\mu}\sum_{l=1}^{\nu}C_{kl}\int_0^1 dx\int_0^1 dy\Theta(xy-K_{\min}^2)\frac{d\bar{n}}{dx\,dy}(e^{-i(t_kx+u_ly)}-1)\right]. \tag{C6}$$

Using a Gaussian approximation [cf. Eq. (12)] one gets

$$\chi_{\mu\nu}(\{x^{(\mu)}\},\{y^{(\nu)}\})=\frac{1}{(2\pi)^{\mu+\nu}}\prod_{k=1}^{\mu}\int_{-\infty}^{+\infty}dt_k\prod_{l=1}^{\nu}\int_{-\infty}^{+\infty}du_l\exp\left[i\sum_{k=1}^{\mu}t_k\left[x^{(k)}-\sum_{l=1}^{\nu}C_{kl}\langle x\rangle\right]\right]$$
$$\times\exp\left[i\sum_{l=1}^{\nu}u_l\left[y^{(l)}-\sum_{k=1}^{\mu}C_{kl}\langle y\rangle\right]\right]$$
$$\times\exp\left[\sum_{k=1}^{\mu}\sum_{l=1}^{\nu}C_{kl}\left(-\tfrac{1}{2}\langle x^2\rangle t_k^2-\tfrac{1}{2}\langle y^2\rangle u_l^2-\langle xy\rangle t_k u_l\right)\right]. \quad \text{(C7)}$$

In order to proceed further one has to define the coefficients C_{kl}. It can be shown that for the case of

$$C_{kl}=1,\quad k=1,\ldots,\mu;\quad l=1,\ldots,\nu \quad \text{(C8)}$$

(which corresponds to $n=\mu\nu$—maximally inelastic event),

$$\chi_{\mu\nu}(\{x^{(\mu)}\},\{y^{(\nu)}\})=\frac{\chi_{0\mu\nu}}{(2\pi)[\mu\nu D_{xy}^2(2\pi\nu\langle x^2\rangle)^{\mu-1}(2\pi\mu\langle y^2\rangle)^{\nu-1}]^{1/2}}$$
$$\times\exp\left\{-\frac{1}{2\nu\langle x^2\rangle}\sum_{k=1}^{\mu}(x-\nu\langle x\rangle)^2-\frac{\langle xy\rangle^2}{2_{\mu\nu}\langle x^2\rangle D_{xy}^2}\left[\sum_{k=1}^{\mu}(x_k-\nu\langle x\rangle)\right]^2\right.$$
$$-\frac{1}{2_{\mu}\langle y^2\rangle}\sum_{l=1}^{\nu}(y-\mu\langle y\rangle)^2-\frac{\langle xy\rangle^2}{2_{\mu\nu}\langle y^2\rangle D_{xy}^2}\left[\sum_{l=1}^{\nu}(y_l-\mu\langle y\rangle)\right]^2$$
$$\left.+\frac{\langle xy\rangle}{\mu\nu D_{xy}^2}\sum_{k=1}^{\mu}\sum_{l=1}^{\nu}(x_k-\langle x\rangle)(y_l-\langle y\rangle)\right\}, \quad \text{(C9)}$$

where all definitions and the parametrization of $\langle x^n y^m\rangle$ and D_{xy}^2 are the same as in Sec. II; $\chi_{0\mu\nu}$ is a normalization constant (every $\chi_{\mu\nu}$ is separately normalized to 1). For $\mu=1$ we recover the formula for hA scattering [Eq. (29)] and for $\mu=\nu=1$ that for hN scattering [Eq. (13)].

As we are interested only in $\chi_{\mu\nu}(x,y)$ where x and y are the energy-momentum fractions of *nuclei A* and *B* deposited in the central region, one has to integrate over $\{x^{(\mu)}\},\{y^{(\nu)}\}$ to get

$$\chi_{\mu\nu}(x,y)=\prod_{k=1}^{\mu}\int_0^1 dx_k\,\delta\left[x-\sum_{i=1}^{\mu}x_i\right]\prod_{l=1}^{\nu}\int_0^1 dy_l\,\delta\left[y-\sum_{j=1}^{\nu}y_j\right]\chi_{\mu\nu}(\{x^{(\mu)}\},\{y^{(\nu)}\}) \quad \text{(C10)}$$

and finally to sum with corresponding nuclear weights $P_{\mu\nu}^{AB}(C_{kl})$:

$$\chi_{AB}(x,y)=\sum_{\mu,\nu}P_{\mu\nu}^{AB}(C_{kl})\chi_{\mu\nu}(x,y)\ . \quad \text{(C11)}$$

In addition to the great complexity of Eq. (C10) the problem of calculating $P_{\mu\nu}^{AB}$ is not yet entirely solved.[46]

[1]Quark Matter 87, Proceedings of the Sixth International Conference on Ultrarelativistic Nucleus-Nucleus Collisions, Nordkirchen, Federal Republic of Germany, 1987, edited by H. Satz, H. J. Specht, and R. Stock [Z. Phys. C **38**, 1 (1988)]; Quark Matter 86, Proceedings of the Fifth International Conference on Ultrarelativistic Nucleus-Nucleus Collisions, Pacific Grove, California, 1986, edited by L. S. Schroeder and M. Gyulassy [Nucl. Phys. **A461**, 1c (1987)]; *Hadronic Matter in Collision*, edited by P. Carruthers and D. Strottman (World Scientific, Singapore, 1986); *Hadronic Matter under Extreme Conditions*, edited by G. M. Zinovjev and W. P. Shelest (Naukova Dumka, Kiev, 1986).

[2]G. N. Fowler, R. M. Weiner, and G. Wilk, Phys. Rev. Lett. **55**, 173 (1985).

[3]G. N. Fowler, A. Vourdas, R. M. Weiner, and G. Wilk, Phys. Rev. D **35**, 870 (1987).

[4]G. Wilk, in *Hadronic Multiparticle Production, Directions in High Energy Physics*, edited by P. Carruthers (World Scientific, Singapore, 1988), p. 410; in *Proceedings of the Shandong Workshop on Multiparticle Production, Jinan, Shandong, China, 1987*, edited by R. C. Hwa and Xie Qu-bing (World Scientific, Singapore, 1988), p. 452.

[5]E. V. Shuryak, Phys. Rep. **61**, 71 (1980).

[6]P. Carruthers and Minh Duong-Van, Phys. Rev. D **28**, 130 (1983); P. Carruthers, in *Local Equilibrium in Strong Interaction Physics (LESIP I)*, edited by D. S. Scott and R. M. Weiner (World Scientific, Singapore, 1985).

[7]G. N. Fowler, E. M. Friedlander, M. Plümer, and R. M. Weiner, Phys. Lett. **145B**, 407 (1984); cf. also M. Plümer, in *Local Equilibrium in Strong Interaction Physics (LESIP I)*, edited by D. S. Scott and R. M. Weiner (World Scientific, Singapore, 1985). $\chi(K)$ is obtained from Table I of Ref. 13 by noting that intervals of energy $W=K\sqrt{s}$ of unequal width correspond to equal number of events (200). Furthermore the normalization has to take into account the fact that in the experiment only events with $K\le 0.72$ were recorded.

[8]D. Brick *et al.*, Phys. Lett. **103B**, 242 (1981); Phys. Rev. D **25**, 2794 (1982).

[9]M. Basile *et al.*, Lett. Nuovo Cimento **41**, 293 (1984), and references therein.

[10]B. Andersson, G. Gustafson, and B. Nilsson-Almqvist, Nucl. Phys. **B281**, 289 (1987); B. Andersson *et al.*, Phys. Rep. **97**, 31 (1983); Z. Phys. C **20**, 317 (1983).

[11]A. Capella *et al.*, Z. Phys. C **3**, 68 (1980); **10**, 249 (1981); **33**, 541 (1987); Phys. Lett. **169B**, 285 (1986).

[12]S. Pokorski and L. Van Hove, Acta Phys. Pol. B **5**, 229 (1974); Nucl. Phys. **B86**, 243 (1975).

[13]For a review and references see S. G. Matinyan, Fiz. Elem. Chastits At. Yadra **16**, 522 (1985) [Sov. J. Part. Nucl. **16**, 226 (1985)]; for most recent results see S. G. Matinyan, E. B. Prokharenko, and G. K. Saviddy, Nucl. Phys. **B298**, 414 (1988); T. Furusawa, *ibid.* **B290**, 469 (1987).

[14]Statistical models are an example of this type. cf. E. L. Feinberg, Usp. Fiz. Nauk **139**, 3 (1983) [Sov. Phys.—Usp. **26**, 1 (1983)]; cf. also *Hadronic Matter under Extreme Conditions*, edited by G. M. Zinovjev and W. P. Shelest (Naukova Dumka, Kiev, 1986).

[15]This approximation is better the higher the energies considered. However, our model relies upon the use of effective structure functions for the gluons [cf. Eqs. (5) and (6)] which are defined in terms of the fractional momenta x and y referring to the infinite momentum frame. Therefore, for consistency we have to neglect masses even at energies where this approximation may not be so good, i.e., in the hadron-nucleus reactions at present energies. As a consequence of this, all invariant energies $\sqrt{s}$ appearing below have been calculated using this approximation.

[16]L. Stodolsky, Phys. Rev. Lett. **28**, 60 (1972); E. Etim, G. Pancheri, and B. Touchek, Nuovo Cimento B **51**, 276 (1967).

[17]G. N. Fowler, E. M. Friedlander, R. M. Weiner, and G. Wilk, Phys. Rev. Lett. **57**, 2119 (1986).

[18]Actually in Refs. 2 and 3 we have used another expression for $\chi(x,y)$ which, because of the Fourier integrals representing the energy-momentum conservation, is equivalent to the present one. It arises when we keep track of the fact that for $x'>x$ and $y'>y$ all $n_i=0$, so that in this region of the phase space $P(n_i=0)=\exp(-\bar{n}_i)$. Of course, both methods lead to identical numerical results, if no further approximations are performed. As a matter of fact, some numerical approximations used in Ref. 3 turned out to be too rough and this, together with a slightly changed input for $\langle K\rangle$ explains the differences in the results for $\chi(K)$ at collider and higher energies. The approximation scheme adopted influences the parametrization used. We have found the present scheme more suitable for generalizations to hA and AA collisions.

[19]S. D. Barton *et al.*, Phys. Rev. D **27**, 2580 (1983).

[20]M. M. Block and R. N. Cahn, Rev. Mod. Phys. **57**, 563 (1985).

[21]cf. P. L'Heureux, B. Margolis, and P. Valin, Phys. Rev. D **32**, 1681 (1985). The use of these functions for low x and M^2 is an ansatz which permits us to make contact with perturbative QCD.

[22]E. M. Friedlander and R. M. Weiner, Phys. Rev. D **28**, 2903 (1983); G. J. Alner *et al.*, Z. Phys. C **33**, 1 (1986); J. Wdowczyk and A. W. Wolfendale, Nuovo Cimento **54A**, 433 (1979); J. Phys. G **10**, 257 (1983).

[23]A clean separation of these two regions of phase space would be highly desirable, both for the purpose of the present investigation as well as for the search of quark-gluon plasma. A quantitative estimate of the "degree of centrality" would be necessary. It is conceivable that the coherence or chaoticity of the emitting source can be helpful in this respect; cf. Ref. 11.

[24]cf. Yu. P. Nikitin and I. L. Rosental, *High Energy Physics with Nuclei, Studies in High Energy Physics Series,* edited by N. M. Queen (Harwood Academic, New York, 1986), Vol. 5, and references therein.

[25]R. Bailey *et al.*, Z. Phys. C **29**, 1 (1985).

[26]W. S. Toothacker *et al.*, Phys. Lett. B **197**, 295 (1987).

[27]W. Busza and A. Goldhaber, Phys. Lett. **139B**, 225 (1984); J. Bowlin and A. Goldhaber, Phys. Rev. D **34**, 778 (1986); M. Jezabek and M. Rozanska, Phys. Lett. B **175**, 206 (1986); S. Frankel and W. Frati, *ibid.* **196**, 399 (1987); A. Capella, J. A. Casado, C. Pajares, A. V. Ramallo, and J. Tran-Thanh Van, Z. Phys. C **33**, 541 (1987); R. C. Hwa and M. S. Zahir, Phys. Rev. D **31**, 499 (1984); C. Y. Wong, *ibid.* **30**, 972 (1984); **32**, 94 (1984); L. P. Csernai and J. I. Kogut, *ibid.* **29**, 2664 (1984); **31**, 2795 (1984); K. Werner, J. Hüfner, M. Kutschera, and O. Nachtmann, Phys. Rev. Lett. **57**, 1684 (1986); S. Date, M. Gyulassy, and H. Sumiyoshi, Phys. Rev. D **32**, 619 (1985); Y. Iga, R. Hamatsu, S. Yamazaki, and H. Sumiyoshi, Prog. Theor. Phys. **77**, 376 (1987); Z. Phys. C **38**, 557 (1988); I. Fukui and A. Hasegawa, Prog. Theor. Phys. **79**, 1283 (1988).

[28]P. M. Fishbane and J. S. Trefil, Phys. Rev. D **3**, 238 (1981).

[29]M. K. Hegab and J. Hüfner, Phys. Lett. **105B**, 103 (1981); Nucl. Phys. **A384**, 353 (1982).

[30]A value of $\gamma>1$ has also been obtained in a different approach by R. Shyam and J. Knoll, Nucl. Phys. **A448**, 322 (1986).

[31]B. Brown *et al.*, Phys. Rev. Lett. **50**, 11 (1983); T. Akesson *et al.*, Z. Phys. C **38**, 397 (1988); cf. also Quark Matter 87, Ref. 1.

[32]S. A. Azimov *et al.*, Izv. Akad. Nauk SSSR, Ser. Fiz. **38**, 898 (1974); Yu. P. Nikitin, I. L. Rosental and F. M. Sergeev, Usp. Fiz. Nauk **121**, 3 (1977) [Sov. Phys. Usp. **20**, 1 (1977)].

[33]Actually we have used for this calculation the approximate scheme developed by J. Gosset *et al.*, Phys. Rev. C **16**, 629 (1977).

[34]R. Albrecht *et al.*, Phys. Lett. B **199**, 297 (1988). It should be recognized that in AA collisions a part of the incident projectile may be stopped completely contributing a low-energy peak to the veto counter (E_{ZDC}) of the WA-80 experiment. Since we are calculating the total energy deposited by the incident projectile, to account for this low-energy peak further assumptions are necessary.

[35]A. Bamberger *et al.*, Phys. Lett. B **184**, 271 (1987).

[36]T. Akesson *et al.*, Z. Phys. C **38**, 383 (1988).

[37]J. D. Bjorken, Phys. Rev. D **27**, 140 (1983).

[38]G. N. Fowler, F. S. Navarra, M. Plümer, A. Vourdas, R. M. Weiner, and G. Wilk, Phys. Lett. B **214**, 657 (1988).

[39]Liu Lian-sou, Meng Ta-chung, Pan Ji-cai, and Peng Hong-an, Phys. Rev. D **37**, 3327 (1988); **38**, 3405 (1988); J. Ranft, *ibid.* **37**, 1842 (1988); N. Pisutova, P. Lichard, and J. Pisut, Phys. Lett. B **172**, 451 (1986); J. Ftacnik, K. Kajantie, N. Pisutova, and J. Pisut, *ibid.* **188**, 279 (1987); G. Baym, P. Brown-Munzinger, V. Ruuskanen, *ibid.* **190B**, 29 (1987); A. D. Jackson and H. Boggild, Nucl. Phys. **A470**, 669 (1987); B. Andersson, G. Gustafsson, and B. Nilsson-Almquist, Nucl. Phys. **B281**, 289 (1987); T. Ochai, Europhys. Lett. **4**, 783 (1987); Prog. Theor. Phys. **78**, 741 (1987); Z. Phys. C **35**, 209 (1987); K. Werner, Phys. Lett. B **208**, 520 (1988); Z. Phys. C **35**, 193 (1988); S. Frankel and W. Frati, Nucl. Phys. **B308**, 699 (1988).

[40]E. V. Shuryak, Phys. Lett. B **207**, 345 (1988).

[41]M. Gyulassy and T. Matsui, Phys. Rev. D **29**, 419 (1984).

[42]Similar results for K (or M) for central collisions of nuclei have been reported from a quite different approach, cf. U.

Ornik, F. W. Pottag, and R. M. Weiner, in *Proceedings of the Conference on Hadronic Matter in Collisions, Tucson, 1988,* edited by P. A. Carruthers and J. Rafelski (World Scientific, Singapore, in press).

[43]A. Capella and J. Tran Thanh Van, Z. Phys. C **38**, 177 (1988), and references therein.

[44]B. Andersson *et al.*, Ref. 39; M. Gyulassy, CERN Report CERN TH 4794/87, 1987; in *Proceedings of the 8th Balaton Conference on Nuclear Physics, 1987,* edited by Z. Fodor (KFKI, Budapest, 1987).

[45]Cai Xu, Chao Wei-qin, and Meng Ta-chung, Phys. Rev. D **36**, 2009 (1987); cf. also Liu Lian-Sou *et al.*, Ref. 39.

[46]I. V. Andreev and A. V. Chernov, Yad. Fiz. **28**, 477 (1978); **28**, 1499 (1978); A. P. Gasparyan, A. P. Cheplakov, and Yu. M. Shabelski, Yad. Fiz. **34**, 1328 (1981) [Sov. J. Nucl. Phys. **34**, 739 (1981)]; A. S. Pak, A. W. Tarasov, W. W. Uzhinskii, and Ch. Tseren, Yad. Fiz. **30**, 102 (1979); **30**, 343 (1979); C. Pajares and A. V. Ramallo, Phys. Rev. D **31**, 2800 (1985); A. M. Braun, Yad. Fiz. **45**, 1625 (1987); **47**, 262 (1988); K. G. Boreszkov and A. B. Kaidalov, *ibid.* **48**, 575 (1988), and references therein.